

Local Remeshing Algorithm for Quasi-Static Crack Propagation

Song, Young Joon
Koh, Byeong Cheon

.....

요 약

균열전파 현상은 항상 형상이 변화하는 대표적인 문제중의 하나이다. 본 연구는 준-정적 균열전파 현상을 해석하기 위하여 델로네이 특성을 이용한 국지 요소재편 알고리즘을 제시하였다. 이 알고리즘은 요소 재편성과 세분화를 모두 수행할 수 있도록 준비되었다. 적용예로 M 적분법을 사용하여 주로 혼합 모우드로 균열이 전파되는 스폐링 현상을 해석하였다.

Abstract

A local remeshing algorithm using Delaunay property is developed for the analysis on the phenomenon of quasi-static crack propagation, which is a typical problem of accompanying constantly varying geometry. The algorithm performs both remeshing and refinement. The use of M-integral is demonstrated to simulate crack propagation under mixed mode with the edge spalling problem.

.....

1. Introduction

Crack propagation has technical importance in many engineering design problems, especially for structures such as bridges or power plants under seismic loading. Because of its nature of constantly varying domain(boundary) with time-marching, it draws attention from many reseachers in the area of numerical analysis.

In general, the following issues are discussed in order to simulate the crack propagation :

- (1) accurate evaluation of the stress intensity factors(SIFs)
 - (2) properly defined crack propagation criterion in mixed mode cracking
 - (3) automatic local/global remeshing algorithm to depict crack propagation process.
- While the first two issues are related to fracture mechanics, the third one is purely to numerical technique. Since crack does not stay on the present position but moves forward according to the combination of SIFs, the simulation of crack propagation must deal with constantly varying geometry. Furthermore the variation

* Korea Military Academy
** Korea Automotive Technology Institute

이 논문에 대한 토론을 1994년 12월 31일까지 본 학회에 보내주시면 1995년 6월호에 그 결과를 게재하겠습니다.

is concentrated in the small region near crack tip. Therefore it can be said that an appropriate scheme representing moving crack front is indispensable to study the phenomenon of crack propagation.

In this regard, Fish and Nath[1] recently proposed the interesting formulation. They considered the cracked body as the superposition of 'a discontinuous finite element field' which contains unconstrained double nodes along the discontinuity with the portions of the finite element mesh 'free of cracks'. Then they simulated crack growth by automatically remeshing the discontinuous field only while keeping the other fixed (or the same as the initial mesh). Pekau and Batta[2] used BEM for the seismic crack propagation analysis of concrete structures, where crack propagation due to dynamic effects is considered.

Provided that the crack advances in the quasi-static manner, the present study is carried out the above issues on crack propagation by using FEM. Especially we have developed the local remeshing scheme in crack front zone. It has been pointed out[3] that Delaunay-Voronoi triangulation method, whose generation algorithm is based on recursive local remeshing schemes, can be one of the candidates. It does need only to define remeshing region for new crack. In fact once the crack increment and its orientation angle are known, it automatically sets the crack front zone and discretizes it. Accurate and easy-to-be-implemented numerical schemes are also discussed for the separation of individual stress intensity factors (SIFs) by using so-called *M*-integral.

2. Mesh generation scheme for crack propagation

2.1 General description of Delaunay triangulation

In recent development of mesh generators [4-12], not only the refining ability but also local remeshing capability is required necessarily for the preparation of such problems as large deformation and crack propagation. In this regard Delaunay triangulation is considered one of the best choices since its generation algorithm is based on recursive local remeshing schemes. For a given set of N distinct points $\{P_n, n=1, 2, \dots, N\}$, Voronoi polygon D_i in 2-dimensional space with respect to point P_i is defined by

$$D_i = \{x : d(x, P_i) < d(x, P_j), \forall j \neq i\} \quad (1)$$

where $d(\dots)$ is an appropriate distance function. In the union D_n of $D_i, i=1, 2, \dots, N$, every vertex point is shared by three polygons, and a Delaunay triangulation is obtained connecting those points. A very important property of Delaunay triangulation is that the hypersphere of Delaunay simplex does not contain any points other than its own vertices, referred to as the property of the *empty sphere* of Delaunay triangulation[13].

When $(k+1)$ th point P is added to the current Delaunay triangulation $T(k)$, revised Delaunay triangulation $T(k+1)$ is obtained as follow.

$$T(k+1) = (T(k) - B(p)) \cup [P, S(p)] \quad (2)$$

where $B(p)$ is a set of triangles whose circumspheres contain the point P , $S(p)$ sequential boundary points of $B(p)$, and $[P, S(p)]$ the triangles generated by connecting lines radially from P to the points on $S(p)$.

In this process, positioning a new point P

has significance in every aspect of the procedure, i.e., 1) locations of the initial nodes delineate problem domain and constitute the boundary triangulation, 2) intervals of the initial nodes provide implicit element density function value at each node of which reciprocal indirectly controls element size, and 3) on the interior, the locations are so determined that densities are checked in the early stage and shape regularities checked in the latter part of mesh development.

Song[3] introduced *adjacency array* NEXT by definition (3) and *adjacency level* as shown in Fig. 1 with a couple of accompanying algorithms[3, 14].

$$\text{NEXT}(i, j) \equiv \text{adjacent element number} \quad (3)$$

facing *i*-the side of the element *j*

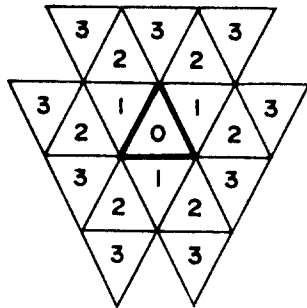


Fig. 1. Adjacency level for regular mesh

Array NEXT provides information about *adjacency* among elements rather than *proximity*, and when used with concept of adjacency level it provides a very effective way of managing screening process to find members of the block B and constructing its boundary loop S. The construction algorithms of the ball B and the loop S are also used in identifying crack front area and in preparing the path of J-integral in the crack tip analysis.

2.2 Refinement scheme

Before entering to the discussion of mesh generation scheme for the crack tip analysis, clear difference between refining and remeshing on a subdomain of the existing mesh should be noticed. *Refining* a subdomain is the process of deviding some of the old elements on the domain, which is equivalent to adding new nodes to the existing set of nodes at devided location of the element sides. None of the existing nodes are eliminated in the process of refinement. On the other hand in *remeshing* a subdomain, the interior nodes of a subdomain are replaced completely by a new set of nodes and elements.

Refinement scheme of a single *core element* [14] in a regular mesh is considered first. Three new nodes are created at midpoints of its lateral sides. The number of elements involved in refining a single core element is four, core element itself and its three immediate adjacent elements. New nodes are inserted into the block one by one, and elements are regenerated according to the generation logic (2). As a result of the refinement the core element is divided into four elements and three adjacent elements are divided into six elements. Refining sequence of a single core element is shown graphically in Fig. 2.

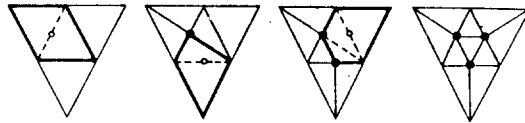


Fig. 2. Refining sequence of a single core element

Refinement of several elements, in clustered or individually, can be dealt with by simple repetition of the same procedure. Special care should be paid on the regularity after refinement. Consider the refinement of a single core

element of Fig. 3. The elements replacing the core element retain the same order of regularity as of the core element. New nodes (mid side nodes of the core element) are connected to five elements, which still can provide good regularity after smoothing. But one of the vertices of every adjacent element is connected to one more element than before refinement. Number of elements connected to the node is likely to increase while refinement continues around it (shown as revision area in Fig. 4). The number of elements connected to a node should be kept less than or equal to 8 to maintain shape regularity. Beyond this number remeshing is necessary to replace degenerated elements. Eliminating the center node in the revision area, unforced insertion of new nodes is carried out until no more node is acceptable.

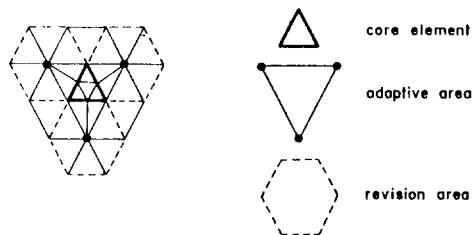


Fig. 3. Refining (adaptive) area and remeshing (revision) area

It has been shown that h-adaptive refinement can be obtained by using the above mentioned scheme [14].

2.3 Remeshing scheme

General mesh scheme for crack analysis problems is such that fine enough meshes are prepared around the crack tip, and the more coarse the further away meshes are from the tip. When the amount of crack advancement δ and its orientation θ with respect to the crack surface (the slit line) are given, remeshing is

necessary so that a new node is positioned at the exact location of new crack tip and the slit line is extended without being intersected by the sides of the surrounding elements. As the direction of the advance is toward where meshes are coarse, mesh gradient in front of the new crack tip becomes steep. In order to ease the severity of density difference, the bigger elements in revision area are refined before remeshing takes place. Following is a summary of the key procedures of producing better remeshing results *in practice* for crack advancement.

1) Remeshing block is determined as shown in Fig. 4. The center of the block is located at the distance of 2.5 times the advancement δ from the old tip in the direction of new crack orientation. The elements whose incenters are within 5δ from the center and whose adjacent levels less than or equal to 8 are collected. Elements on the back half plane divided by the normal to the crack orientation are excluded from the block.

2) Elements whose minimum side length is less than 1.8δ are refined before remeshing, which are located further away from the tip in general (Fig. 4). The process adjusts the density function values much less, almost in half, than the previous ones for nodes on the peripheral of the remeshing block. The adjust-

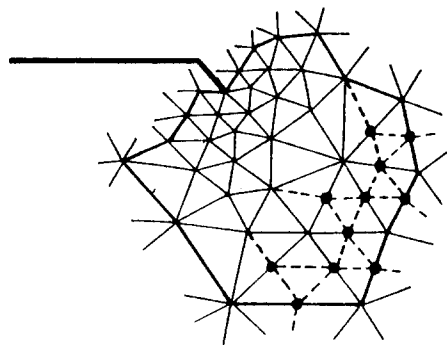


Fig. 4. Remeshing block and *a priori* refining

ment enables the remeshing to provide smooth element gradient between the crack tip area and the exterior of the block.

3) After eliminating all the interior nodes of the block, five new nodes are inserted consecutively at the distances incremented by 0.5δ in the slit direction. The first two nodes delineate the extended slit. One extra node is put at mid-point of the slit extension for the better path of J-integral in the new crack orientation. The last three nodes are inserted to provide fine enough elements ahead of the crack tip. After forced insertions of 5 nodes, unforced insertions follow as long as the requested conditions for shape regularity and density of the elements are not violated. Fig. 5 shows a sequence of insertions.

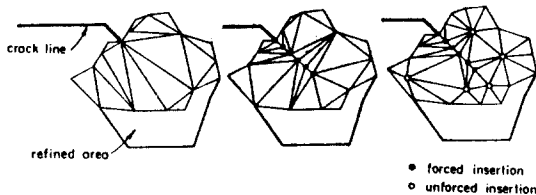
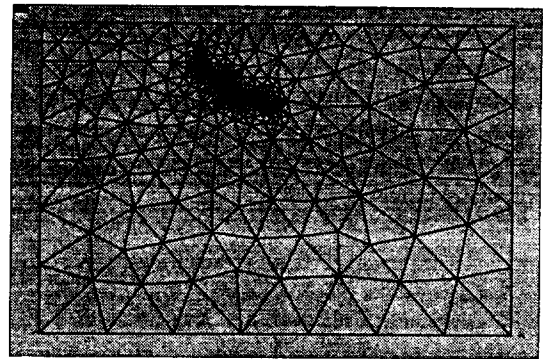


Fig. 5. Insertion of nodes for slit extension

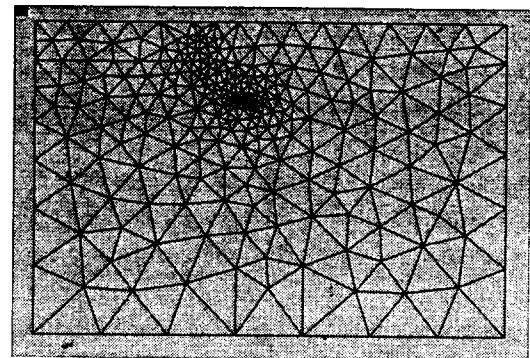
4) Smoothing is carried out at every revision of the crack tip area using the concept of barycenter[14, 15]. Smoothing due to crack tip remeshing includes such nodes as those generated in *a priori* refinements, connected to the refined elements, generated during remeshing the block, and those of the adjacent elements of the block. Global smoothing does not always provide favorable situation. Local smoothing is necessary as well as global one. For example repeated application of global smoothing tends to make large elements even larger than before smoothing. Here local smoothing is used extensively.

5) When the slit line is developed for a cer-

tain length or number of elements is too much on the free edge of the crack, the whole slit line can be rediscrretized as shown in Fig. 6.



before rediscrretization



after rediscrretization

Fig. 6. Rediscrretization of slit line

3. Determination of the angle of crack orientation

3.1 Evaluation of Individual SIFs

Many ways to evaluate the crack extension force are suggested. Among them, J-integral proposed by Rice is now widely used because it gives robust and accurate solutions regardless of mesh description,

The energy release rate $E(\varrho)$ is defined as the rate of the total potential energy due to crack extension, and can be written[16, 17] as

$$E(\ell) = -\frac{d}{d\ell} \left(\int_{\Omega} W \, d\Omega \right)$$

when the boundary of the domain except crack surface is fixed. Here ℓ denotes crack length and thus $d/d\ell$ implies the direction of crack propagation. It also has been known that the J-integral J has the relation

$$E(\ell) = J = \int_{\Gamma} \{ W_n - T_i \partial u_i / \partial \ell \} \, d\Gamma \quad (4)$$

When the crack turns or curves under mixed mode cracking, J-integral (4) can be computed easily by using the chain rule

$$d/d\ell = d/dx \, dx/d\ell + d/dy \, dy/d\ell$$

The above J-integral method provides a good approximation on the overall strength of the crack-tip singularity. However it is not obvious to find the opening and the shearing effects from the overall solution in the case of mixed mode cracking. In order to predict the individual SIF's from the overall intensity, M-integral proposed by [18] has been adopted. It is defined as :

$$M\{\mathbf{u}, \mathbf{u}^a\} = \int_{\Gamma} \{ 1/2(\sigma_{ij} \varepsilon_{ij}^a + \sigma_{ij}^a \varepsilon_{ij}) - (T_i \partial u_i^a / \partial \ell + T_i^a \partial u_i / \partial \ell) \} \, d\Gamma$$

where \mathbf{u} , \mathbf{u}^a are the solutions of the actual stress field and an auxiliary stress field, respectively. Since the above M-integral has a similar form to J-integral, the same J-integral algorithm can be enough for their implementation. Note that M-integral has the orthogonal property of

$$M\{\mathbf{u}^I, \mathbf{u}^{II}\} = 0$$

where \mathbf{u}^I and \mathbf{u}^{II} are the displacements in the stress fields of pure modes K_I and K_{II} , re-

spectively. Since the actual field solution \mathbf{u} is written as the sum of, i.e. $\mathbf{u} = \mathbf{u}^I + \mathbf{u}^{II}$, the following holds :

$$\begin{aligned} M\{\mathbf{u} = \mathbf{u}^I + \mathbf{u}^{II}, \mathbf{a}^I\} &= C K_I A_I \\ M\{\mathbf{u} = \mathbf{u}^I + \mathbf{u}^{II}, \mathbf{a}^{II}\} &= C K_{II} A_{II} \end{aligned}$$

where C is material proportionality, \mathbf{a}^I and \mathbf{a}^{II} are auxiliary pure mode solutions corresponding to SIFs A_I and A_{II} , respectively. Here the solutions of the singular crack tip field in linear elastic fracture are chosen such that A_I or $A_{II} = 1$. Assumed that the singularity is dominant near the crack tip, the integral path is selected as close as possible to crack tip. Its detail derivation can be referred in [18].

3.2 Determination of crack orientation angle

In general, the crack under mixed mode changes its direction according to certain combination of individual SIFs, provided that the crack instability is formed in the region dominated by crack tip singularity. As for determining the crack orientation angle, the criteria of the maximum tensile stress or the maximum strain energy density are mostly used.

Here is adopted the maximum tensile strain criterion [15], which postulates that the circumferential strain ε_{θ} at the crack tip becomes the maximum. Indeed,

$$\varepsilon_{\theta} = K_I / \sqrt{(2\pi r)} f^I(\theta) + K_{II} / \sqrt{(2\pi r)} f^{II}(\theta)$$

where θ is the angle from the crack orientation line. f^I and f^{II} are obtained from linear elastic K_I and K_{II} crack solutions, respectively, so that

$$f^I(\theta) = 1 / (4E) \{ (3 - 5\nu) \cos(\theta / 2) + (1 + \nu) \cos(3\theta / 2) \}$$

$$f^{II}(\theta) = -1 / (4E) \{ (3 - 5\nu) \sin(\theta / 2) + 3(1 + \nu) \sin(3\theta / 2) \}$$

Therefore the orientation angle θ can be determined such that ϵ_θ be the maximum, or $\partial\epsilon_\theta / \partial\theta = 0$ which leads to a cubic equation

$$2\nu K_I \tan^3(\theta / 2) + 2(3 + 4\nu) K_{II} \tan^2(\theta / 2) - (3 + \nu) K_I \tan(\theta / 2) - (3 + \nu) K_{II} = 0$$

Note that the above equation implies that $\theta = 0$ when $K_{II} = 0$, θ is negative when $K_{II} > 0$, and θ is positive when $K_{II} < 0$.

4. Numerical examples

4.1 Edge-cracking problem

As an example, an edge cracking problem of homogeneous brittle material is chosen, whose technical importance is mentioned as for edge-machining in Thouless et al[19]. Fig. 7 shows a standard spalling problem where a cracked body is under a compressive load on the top of crack flank. The lower side wall is considered as fixed.

In general, this problem is essentially under the mixed mode cracking. Lateral compressive load causes not only the shearing of crack flank but the opening due to the offset of a loading point from the neutral line where pure shearing mode (K_{II}) exists. One of important observations in such problems is that the edge-crack propagates with a constant width of crack flank (characteristic depth) from the side surface during steady crack growth stage. The spalling mechanism is well discussed by Thouless et al. in [19].

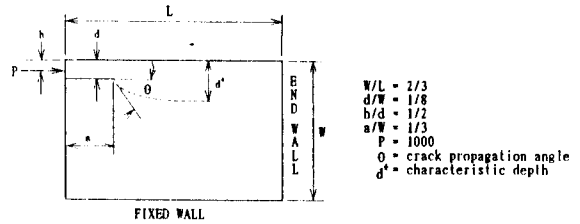


Fig. 7. Numerical model for a spalling problem

4.2 Numerical model

Here the numerical analysis is performed to find crack tip points due to crack advance. As crack tip advances, crack may change its orientation and eventually keeps the characteristic depth when it reaches the steady crack-growth state.

The following process is employed for the numerical experiments :

- Step 1 : Define and new crack tip region
- Step 2 : Rediscretize the crack region
- Step 3 : Solve the stress analysis
- Step 4 : Compute individual stress intensity factors
- Step 5 : Evaluate the crack-advancing angle
- Step 6 : Repeat 1-5 until the steady state reaches

Although the crack growth is often dynamic, it is assumed quasi-static in the numerical model. The crack instability is assumed in every crack increment ; that is, the overall singularity strength at the crack tip is bigger than the fracture toughness of the material. For the assumed crack increments, the orientation of crack-advancing angle is evaluated in step 5. Here the increment was determined as 'assumed length' with a small value (1/18 of the initial crack length) for our computational convenience. In order for the increment to have the meaning, it may be determined with the time integration steps.

4.3 Numerical results

Two cases of edge-cracking problems are considered; one with end wall of free boundary and another with end wall of constraint in x-direction. Indeed it appears that boundary conditions of end wall affected the crack tip orientation when the tip becomes closer to the end wall. The dimensions of the problem considered are shown in Fig. 7.

The strength of stress intensity factors are dictated by load P and its loading line (or the distance from the free surface) h . Indeed it is discussed in [19] that the stress intensity factors in these problems are dependent on the ratio between loading line (h) and flank width (d). Pure opening mode ($K_{II}=0$) appears at between $h/d=5$ and 6.1 according to the end wall conditions by using numerical solutions.

Tables 1 and 2 demonstrate that the SIFs and the orientation angle with respect to crack increments in case of free end wall and sliding wall, respectively. While the crack advancements at the beginning stage are very similar in both cases, they show discrepancy when the crack develops enough. At the beginning the crack starts to grow downward steeply ($52^\circ-53^\circ$) from the free upper side, when the strong positive shear mode exists. The crack of free wall tends to keep the angle about 30° and thus the slanted crack is developed as the crack grows further (Fig. 8). Notice that the shear mode K_{II} almost vanishes, which means that crack advances with the same orientation angle with the previous step. This result is quite different to the discussion made in [19]. It may come from the finite size effect of the domain. Indeed if the straight crack of $d/h=5$ in free end wall is considered initially, the crack advances straight (0°) to keep its characteristic depth. Otherwise, there seems to be no way to induce the negative

shear mode, since lower side wall is the only boundary to resist the compressive load. The overall crack intensity also keeps increasing as the crack grows.

The crack of sliding wall has the tendency to constantly turn its angle and eventually reaches the 'steady' state (Fig. 8) where the maximum crack depth is obtained as $(d/h)_{\max}=4.72$. However notice that the overall crack singularity becomes to lose its intensity as the crack grows, which means that the crack advancement may stop at a certain point. Indeed when the crack is kept to grow until it reaches to the side wall, it is found that the problem becomes simply to the standing column subjected to compression because the movement in x-direction is not allowed.

Fig. 9 and 10 show the distribution of equivalent stress in case of sliding and free end walls, respectively

Table 1. The SIFs and the orientation angle w.r.t. crack increment step (free end wall)

Step	Tip Angle ($^\circ$)	Stress Intensity Factors		
		Overall	K_I	K_{II}
1	0	15712	9236	12706
2	-45.3	17007	16331	1058
3	-52.6	16556	16168	-1578
4	-41.5	16848	16579	-138
5	-40.6	16319	16508	-565
10	-27.1	18534	18722	-302
15	-29.3	20608	20825	-515
20	-29.0	23660	23756	-964

Table 2. The SIFs and the orientation angle w.r.t. crack increment step (sliding end wall)

Step	Tip Angle ($^\circ$)	Stress Intensity Factors		
		Overall	K_I	K_{II}
1	0	15396	8656	12457
2	-45.5	15350	15078	1210
3	-54.5	15883	15133	-2356
4	-38.1	14404	14020	232
5	-40.1	14704	15470	-1355
10	-25.7	14019	14087	-986
15	-5.6	13265	13336	-500
22	-0.14	12155	12329	-93

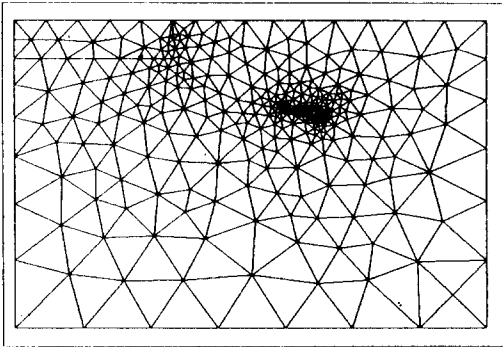


Fig. 8. Crack growth of the model(sliding end wall)

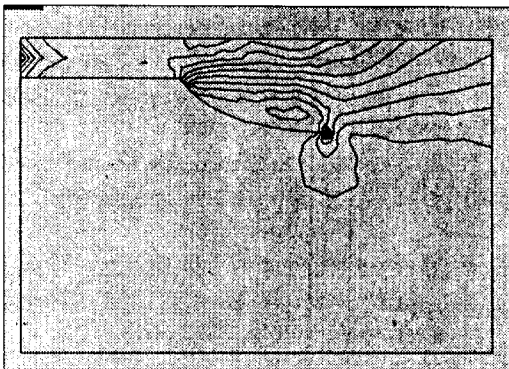


Fig. 9. Distribution of equivalent stress(sliding end wall)

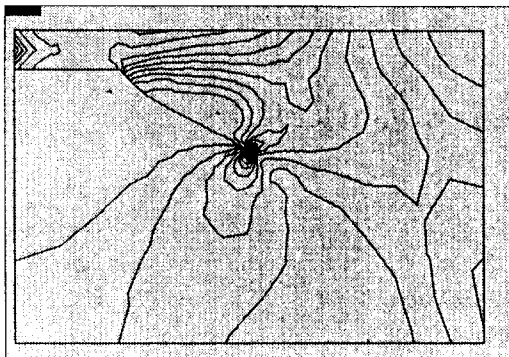


Fig. 10. Distribution of equivalent stress(free end wall)

5. Conclusions

In the present study, the numerical schemes to simulate crack propagation are proposed :

the recursive local remeshing scheme by using the Delaunay triangulation to simulate constantly varying domain and accurate evaluation of SIFs by using M-integral. The use of the adjacency array NEXT and the suggested algorithms make it possible to accomodate changing crack tip area by identifying remeshing block B and its boundary nodes S instantaneously when needed anywhere in the domain. The local remeshing scheme is especially useful in the large deformation problems such as back extrusion where the deformation of the given geometry(or boundary) is concentrated in a local region.

However the discussions on crack propagation here are limited to quasi-static problems. Since in reality the brittle crack propagates dynamically, further development must be able to deal with the accompanying dynamic effect which leads that time integration scheme is necessary. To estimate the accurate time increment, the predictor-corrector algorithm may be needed. In addition, the generalizations of J-integral and M-integral are also required for evaluating correctly SIFs by the effects of dynamic load.

References

1. J. Fish and A. Nath, "Adaptive and hierarchial modelling of fatigue crack propagation", *Int. J. Num. Meth. Eng.*, vol. 36, 2825-2836(1993)
2. O. A. Pekau and V. Batta, "Seismic crack propagation analysis of concrete structures using boundary elements", *Int. J. Num. Meth. Eng.*, vol. 35, 1547-1564(1992)
3. Y. J. Song, "A simple algorithm for maintaining adjacency and remeshing process in Delaunay-Voronoi triangulation", *J. Comp. Struct. Eng. Inst. Korea*, 3, Vol. 6, 99-112 (1993)

4. A. R. Diaz, N. Kikuchi and J. E. Taylor, "Design for optimal grid for finite element methods", *J. Struct. Mech.*, 11(1983)
5. M. C. Rivara, "Algorithms for refining triangular grids suitable for adaptive and multigrid techniques", *Int. J. Num. Meth. Eng.*, vol. 20, 745-756(1984)
6. W. H. Frey, "Selective refinement : A new strategy for automatic node placement in graded triangular meshes", *Int. J. Num. Meth. Eng.*, vol. 24, 2183-2200(1987)
7. W. J. Schroeder and M. S. Shephard, "Geometry-based fully automatic mesh generation and Delaunay triangulation", *Int. J. Num. Meth. Eng.*, vol. 26, 2503-2515(1988)
8. S. W. Bova and G. F. Carey, "Mesh generation/refinement using fractal concepts and iterative function systems", *Int. J. Num. Meth. Eng.*, vol. 33, 287-305(1992)
9. B. P. Johnston and J. M. Sullivan Jr, "Fully automatic two-dimensional mesh generation using normal offsetting", *Int. J. Num. Meth. Eng.*, vol. 33, 425-442(1992)
10. C. K. Lee and S. H. Lo, "An automatic adaptive finite element procedure for 2D elastostatic analysis", *Int. J. Num. Meth. Eng.*, vol. 35, 1967-1989(1992)
11. T. Bellytschko and M. Tabbara, "H-Adaptive finite element method for dynamic problems with emphasis on localization", *Int. J. Num. Meth. Eng.*, vol. 36, 4245-4265(1993)
12. R. V. Nambier, R. S. Valera and K. L. Lawrence, "An algorithm for adaptive refinement of triangular element meshes", *Int. J. Num. Meth. Eng.*, vol. 36, 499-509(1993)
13. B. Delaunay, "Sur la sphere vide", *Bull. Acad. Sci. USSR*, 117, 793-800(1934)
14. Y. J. Song, "Refinement scheme by using Delaunay properties in adaptive finite element implementation", *J. Korea Military Academy*, vol. 45, 475-498(1993)
15. P. L. George, *Generation automatique de maillages*, Masson, 1990
16. J. R. Rice, "A path independent integral and its approximate analysis of strain concentration by notches and cracks", *J. Appl. Mech.*, vol. 35, 379-386(1968)
17. M. E. Gurtin, "On the energy release rate in quasi-static elastic crack propagation", *J. Elast.*, vol. 9, 187-195(1975)
18. F. H. K. Chen and R. T. Shield, "Conservation laws in elasticity of the J-integral type", *ZAMP*, vol. 28, 1-22(1977)
19. M. D. Thouless, A. G. Evans, M. F. Ashby, and J. W. Hutchinson, "The edge cracking and spalling of brittle plate", *Acta Metal.*, vol. 35, 1333-1341(1987)

(接受 : 1994. 7. 14)